

Three-dimensional ab initio simulation of laser-induced desorption of NO from NiO(100)

Dominik Kröner^{a,1}, Imed Mehdaoui^{a,b}, H.-J. Freund^a, Thorsten Klüner^{b,*}

^a Fritz-Haber-Institut der Max-Planck-Gesellschaft, Faradayweg 4-6, D-14195 Berlin, Germany

^b Universität Oldenburg, Theoretische Physikalische Chemie, D-26111 Oldenburg, Germany

Received 9 August 2005

Available online 23 September 2005

Abstract

Laser-induced desorption of NO molecules from a NiO(100) surface is studied on an ab initio level. Based on ab initio NiO-cluster calculations a three-dimensional potential energy surface was constructed for the electronic ground and a representative excited state. Quantum wave packet calculations on these surfaces allow the simulation of experimental velocity distributions of the desorbed NO molecules. Analysis of the wave packet dynamics demonstrates that the experimentally observed bimodality of the velocity distributions is caused by a bifurcation of the wave packet on the excited state potential, where the molecular motion parallel to the surface plays a decisive role.

© 2005 Elsevier B.V. All rights reserved.

1. Introduction

Laser-induced desorption of small molecules from surfaces represents the most simple model scenario of photochemical reactions on surfaces. In the last decade, sophisticated quantum state resolved experiments as well as their corresponding theoretical interpretation [1–4] have been reported. In particular, UV laser-induced desorption of NO from a NiO(100) surface represents an experimentally well-studied system giving rise to a theoretical debate recently. In 1998 Klüner et al. interpreted the experimentally obtained bimodal velocity distributions (cf. Fig. 1) in this system being due to a bifurcation of a wave packet in the intermediate electronically excited state potential energy surface (PES) [5]. This interpretation has recently been questioned in a semi-classical investigation on empirical PESs of Bach et al. [6] in which no pronounced bimodality of the final state distributions has been obtained, and a late desorption channel was found in contrast to the aforemen-

tioned study. In this Letter we will demonstrate, that the application of empirical PESs is not realistic enough. Further, we will clarify the mechanistic understanding on the basis of quantum dynamical wave packet studies on three-dimensional ab initio PESs for the electronic ground and a relevant excited state, respectively, which have been calculated for the first time on a full ab initio level. Although no perfect agreement with experimental results is achieved in the present study, we will provide fundamental insight into the physical mechanism of laser-induced desorption.

2. Model and theory

The NiO(100) surface is modeled by a NiO₅Mg₁₃¹⁸⁺ cluster which is embedded in a Madelung field of 2906 point charges in order to simulate the correct electrostatic field above the oxide surface. In the minimum energy geometry of the electronic ground state the N-atom of the NO molecule is located atop of the Ni²⁺ cation at a distance of 1.99 Å, see Fig. 2. The NO molecule is tilted by 58° towards the surface normal with its O-atom pointing towards the next Ni-atom (here approximated by a Mg-atom) of the cluster. This is in reasonable agreement with recent experimental values of 59° and 1.88 ± 0.02 Å [7,8].

* Corresponding author. Fax: +49 441 798 3964.

E-mail address: Thorsten.Kluener@uni-oldenburg.de (T. Klüner).

¹ Present address: Universität Potsdam, Theoretische Chemie, Karl-Liebknecht-Strasse 24-25, D-14476 Potsdam-Golm, Germany.

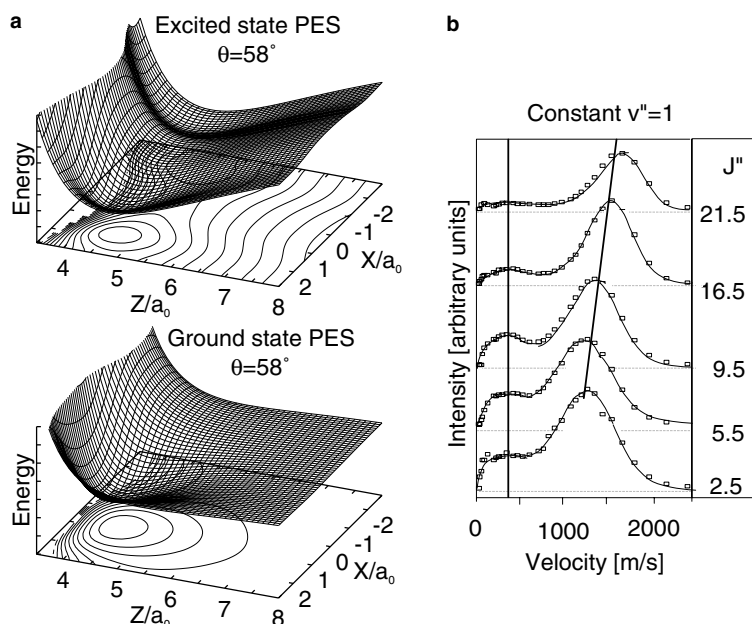


Fig. 1. (a) Two-dimensional plots of the excited (top) and ground state (bottom) PES. (b) Experimental velocity distributions of rotationally (J'') excited NO molecules after laser-induced desorption from NiO(100) [2]. For a given v'' a coupling of rotation and translation is observed for molecules desorbing with high velocities (fast channel).

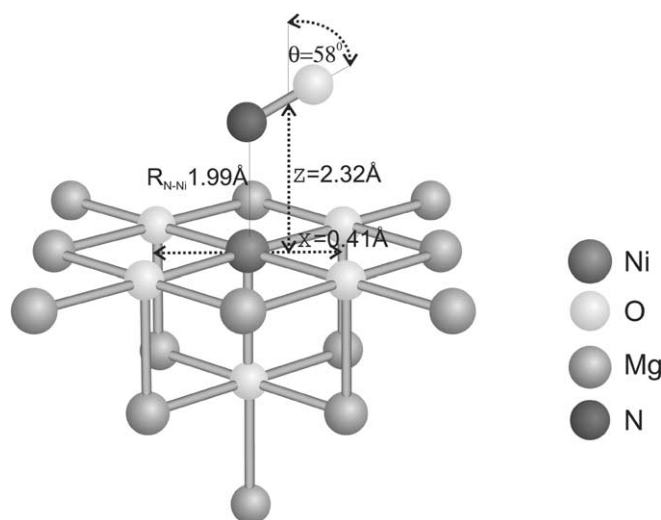


Fig. 2. Minimum energy geometry of NO on the $\text{NiO}_5\text{Mg}_{13}^{18+}$ cluster.

Three degrees of freedom of the NO molecule were considered in our calculations (the $\text{NiO}_5\text{Mg}_{13}^{18+}$ cluster is assumed rigid): (1) The desorption coordinate Z , being the distance between the NiO surface and the center of mass of NO, (2) the lateral coordinate X , describing the motion of the center of mass of the NO molecule along the Ni–Ni-surface diagonal, (3) the polar angle θ between the NO-bond and the surface normal, where for $\theta = 0^\circ$ the NO-bond is parallel to the surface normal with the N-atom pointing towards the surface.

Along these three degrees of freedom the PES of the energetically lowest doublet state, the electronic ground state, was obtained by single-point calculations at the CASSCF

and CASPT2 level of theory. In the CASSCF(3,3) calculations the active space included Ni 3d(z^2), 3d($x^2 - y^2$) orbitals and the NO $2\pi^*(z)$ antibonding orbital with three active electrons. In the following CASPT2 calculation, the valence electrons in the Ni 3d, N 2sp and O 2sp (surface and NO) orbitals were correlated. For the CASSCF–CASPT2 calculations we used the MOLCAS 5.4 package [9].

The contraction scheme of the 332 basis functions will be published elsewhere [10]. For the minimum energy geometry the counterpoise corrected [11] NO-cluster adsorption energy at CASPT2 level is -0.34 eV which underestimates the experimental bond strength of -0.57 ± 0.04 eV [12] due to the limited cluster size, the finite one-particle basis and the approximate treatment of electron correlation. For a detailed discussion the reader is referred to [13]. The NO bond length was optimized to give the lowest NO-cluster adsorption energy. Since NO vibration has been found to be decoupled from translation experimentally, the NO bond length was kept fixed at $R_{\text{NO}} = 1.170$ Å ($2.211a_0$) which is in good agreement with previous theoretical calculations [13].

The electronically excited states relevant for the DIET process are charge transfer states where one electron is transferred from the cluster (either from O 2p or Ni 3d) to the $2\pi^*$ orbitals of the NO molecule resulting in an $\text{NO}^-(\text{NiO}^+)$ -like intermediate [14]. Although more than one electronic excited state might be involved in the DIET process, only the lowest sextet charge-transfer state was calculated by valence configuration interaction (VCI) with the active space consisting of the O 2sp- (first layer of O-ions), Ni 3d-, and NO 3 σ^- , 4 σ^- , 5 σ^- , 1 π^- and $2\pi^*$ -orbitals using the Bochum suite of ab initio programs [15–18].

Previous studies imply that the consideration of only one representative excited state turns out to be a reasonable approximation due to the topological similarity of various charge transfer states of the NO/NiO(100) system [19]. Details on the ab initio calculation of the electronically excited state will be described elsewhere [10]. Briefly, the minimum of the three-dimensional excited state PES is located at a smaller NO surface distance ($Z = 2.12 \text{ \AA}$) than the minimum of the ground state potential ($Z = 2.32 \text{ \AA}$). This fact would suggest an Antoniewicz-like desorption mechanism [20] in a one-dimensional (i.e., Z) model, but due to the high dimensionality of the PES the mechanism is indeed more complex. Furthermore, the NO^- species in the excited state prefers an almost horizontal position on the surface ($\theta = 88^\circ$) and its center of mass is shifted along the lateral coordinate to $X = -1.32 \text{ \AA}$. This is in contrast to previous studies, in which the lateral translation coordinate X has been neglected [5].

For both electronic states a total of more than 800 single-point calculations along the three coordinates Z , X and θ were performed. In order to obtain three-dimensional PESs these sets of points were analytically fitted. Two-dimensional cuts of the three-dimensional PES for the ground and electronic excited state are presented in Fig. 1. Details on the parameters of the analytical fits will be published elsewhere [10]. The nuclear dynamics on the PESs of the ground and the excited state were simulated by three-dimensional wave packet calculations on a grid of $128(X) \times 80(\theta) \times 256(Z) = 2621440$ points. In all calculations the time evolution operator was approximated by the second order split-operator method proposed by Feit and Fleck [21] using time steps of 10 or $50\hbar/E_h$ for the excited and ground state potential, respectively. The initial wave function of the simulation is the energetically lowest rovibrational eigenfunction ψ_0 of the electronic ground state PES. The excitation of the NO/NiO system is modeled by transferring ψ_0 vertically onto the excited state potential where it is propagated for specific residence times τ_n . To simulate the desorption process, the wave packet is, then, vertically transferred back onto the ground state, where it is propagated under the influence of the ground state PES until final time t_f . Here $t_f = 10 \text{ ps}$ was sufficient to ensure convergence for asymptotic observables of each quantum trajectory. The part of the wave packet in the far asymptotic region of the ground state potential corresponds to desorbed NO molecules.

State resolved velocity distributions are obtained from momentum space probability densities in the asymptotic region for each rotational state J . Because a single wave function cannot describe an ensemble of molecules in a dissipative scenario the incoherent average scheme for different residence times τ_n of N quantum trajectories proposed by Gadzuk [22] was applied. In this method, the expectation values or distributions of desired observables are averaged with an exponential factor, where the resonance lifetime τ is the only semi-empirical parameter. In order to simulate the experimentally observed velocity

distributions of the desorbing NO molecules, a resonance lifetime τ of 48.4 fs ($2000\hbar/E_h$) has been used resulting in desorption probabilities comparable to experimental findings [23]. Convergence of the Gadzuk-averaging was obtained for $N = 80$ quantum trajectories.

3. Results

The averaged velocity distributions for selected rotational quantum numbers J are presented in Fig. 3a. They exhibit a pronounced bimodality with a slow desorption channel at about 300–400 m/s and a fast desorption channel at 1300–1600 m/s. In comparison to the experimental velocity distributions (Fig. 1), with a slow desorption channel in the range of about 200–500 m/s and a fast desorption channel in the range of about 1200–1600 m/s, our theoretical results are in the correct velocity range and exhibit the observed bimodality [2]. For the fast desorption channel our theoretical results show a coupling of rotation and translation, yet, the correlation between the rotational

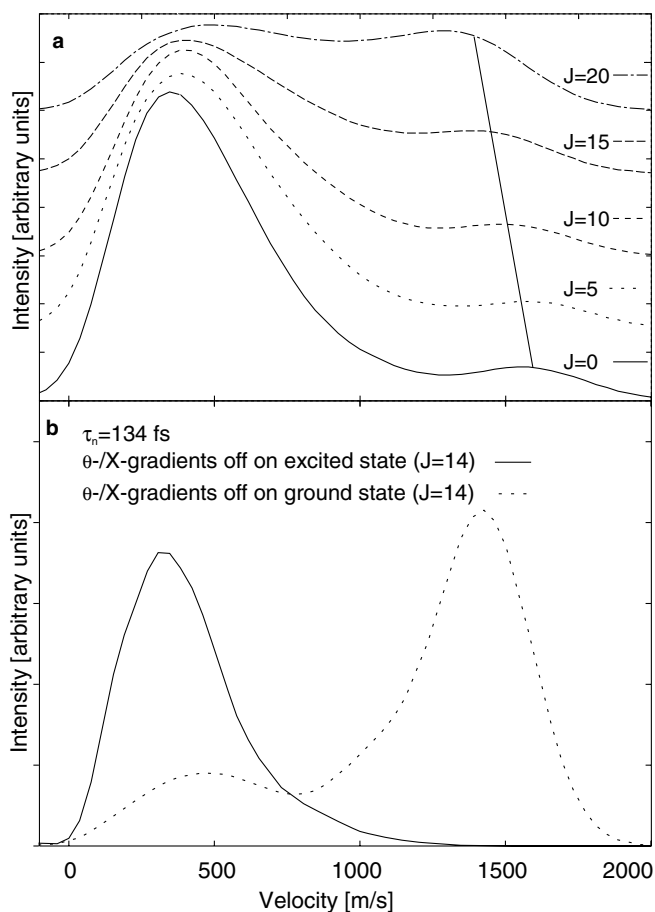


Fig. 3. (a) Averaged velocity distributions for a resonance lifetime $\tau = 48.4 \text{ fs}$ ($2000\hbar/E_h$) and rotational quantum states $J = 0, 5, 10, 15, 20$. The fast desorption channel exhibits a coupling to the rotational quantum states J as indicated by the solid line. (b) Final velocity distributions for a representative residence time $\tau_n = 134 \text{ fs}$ ($5520\hbar/E_h$) for the rotational quantum state $J = 14$ after turning off θ - and X -gradients in the ground state (dashed line) or in the excited state (solid line) PES.

quantum states J and the fast desorption channel are reversed compared to the experimental observations. Furthermore, also the intensities of the fast and slow desorption channel are reversed to the experimental findings. Whether this discrepancy could be due to the omission of the azimuthal angle ϕ which, in reality, contributes to the rotational quantum state, is currently investigated in 4D-studies.

To elucidate the origin of bimodal velocity distributions we performed additional calculations in which both gradients of either the ground state or the excited state potential are set to zero for the polar angle θ and the lateral coordinate X . These calculations show that a bimodal distribution is only observed if the X - and θ -gradients of the excited state PES are non-zero (see Fig. 3b). Thus, we can conclude that the dynamics on the excited state PES is responsible for the observed bimodality.

In order to gain further insight, an extensive analysis of the time evolution of the initial wave packet on the excited state PES was performed. As an example, a characteristic quantum trajectory (residence time of $\tau_n = 134$ fs) is considered. The velocity distribution and a two-dimensional contour plot of that wave packet are shown in Fig. 4. As can be seen in Fig. 4a, after a residence time of $\tau_n = 134$ fs, the wave packet in the excited state is moving towards the surface and the velocity distribution exhibits bimodal characteristics. Close examination of the two-dimensional contour plot of the wave packet in Figs. 4b proves that the wave packet is divided at $Z \approx 4.15a_0$ into two partial wave packets separated by the lateral coordinate X . This is caused by the topology of the excited state PES leading to two pathways for the wave packet. Since the two partial wave packets differ in their molecule–surface distance Z they will result in a bimodal velocity distribution after relaxation to the ground state and dissociation. This is, of course, only valid if the ground state PES has no or very little influence on the shape of the wave packet in momen-

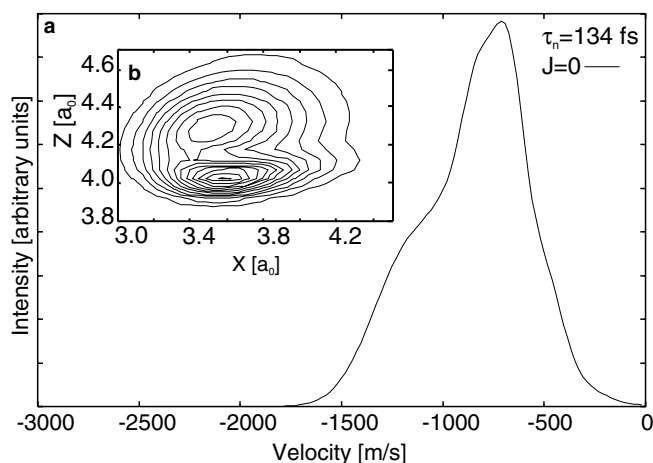


Fig. 4. (a) Velocity distribution of the wave packet on the excited state PES for a specific residence time $\tau_n = 134$ fs ($5520\hbar/E_h$) and rotational quantum number $J = 0$. Inset (b) shows a 2D contour plot of the wave packet on the excited state PES after a residence time $\tau_n = 134$ fs.

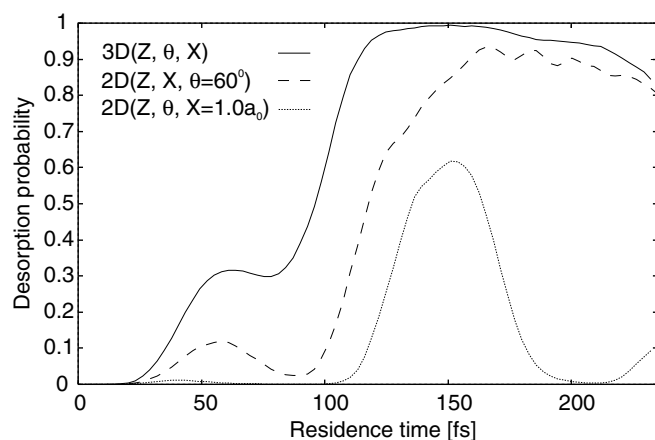


Fig. 5. Desorption probability as a function of the residence time for the three-dimensional (Z, θ, X) (solid line), the 2D (Z, θ) (dotted line), and 2D (Z, X) (dashed line) wave packet study.

tum space after relaxation as can be deduced from results presented in Fig. 3b.

Finally, we want to point out the importance of the lateral coordinate X for the desorption process. Fig. 5 shows the desorption probability as a function of the residence time τ_n for the discussed three-dimensional wave packet simulations and two two-dimensional wave packet simulations including the desorption coordinate Z and either the polar angle θ or the lateral coordinate X . If only Z and θ are considered in the simulations, almost no desorption occurs for residence times $\tau_n = 0$ –100 fs which are relevant for the incoherent averaging scheme. Noticeable desorption is found only for residence times greater than 100 fs. Yet, a remarkable increase of the desorption probability is observed if the lateral coordinate X is included instead of the polar angle θ . In this case, desorption starts at a residence time of about 20 fs and shows similar characteristics as in the three-dimensional wave packet study, i.e. one small peak at $\tau_n \approx 60$ fs followed by a strong increase of the desorption probability for $\tau_n > 100$ fs.

4. Conclusions

In conclusion, we presented a complete three-dimensional quantum simulation of the laser-induced desorption of NO from NiO(100) on a first principles basis. In contrast to Bach et al. [6] the velocity distributions of the desorbed NO molecules are in good agreement with the experimental results and further no ‘late’ desorption channel was observed in our calculations even though each quantum trajectory was propagated until its desorption yield was converged ($t_f = 10$ ps). This clearly points out the necessity of reliable ab initio PESs in the simulation of laser-induced desorption. The different results found in the two studies are due to substantial differences in the topology of the PESs used. The main experimental features are reproduced. The velocity distributions are in the correct velocity range and exhibit the experimentally observed bimodality. Even though the intensities of the two

desorption channels are reversed and the velocity of the fast desorption channel is decreasing with increasing J in contrast to experimental findings, the coupling of rotation (θ) and translation (Z) was reproduced. The origin of the bimodality in the velocity distributions was identified to be caused by a splitting of the wave packet in the lateral coordinate X on the electronically excited PES into a ‘fast’ and a ‘slow’ part.

Therefore, new physical insight into microscopic understanding of laser-induced desorption has been obtained which lays the foundation for future four-dimensional studies and more detailed experiments.

Acknowledgements

Fruitful discussions with M. Pykavy and S. Borowski and financial support by the Deutsche Forschungsgemeinschaft (SPP1093) are gratefully acknowledged.

References

- [1] H. Guo, P. Saalfrank, T. Seideman, *Prog. Surf. Sci.* 62 (1999) 239.
- [2] T. Mull, B. Baumeister, M. Menges, H.-J. Freund, D. Weide, C. Fischer, P. Andresen, *J. Chem. Phys.* 96 (1992) 7108.
- [3] S. Thiel, M. Pykavy, T. Klüner, H.-J. Freund, R. Kosloff, V. Staemmler, *Phys. Rev. Lett.* 87 (2001) 077601.
- [4] S. Borowski, T. Klüner, H.-J. Freund, *J. Chem. Phys.* 119 (2003) 10367.
- [5] T. Klüner, H.-J. Freund, V. Staemmler, R. Kosloff, *Phys. Rev. Lett.* 80 (1998) 5208.
- [6] C. Bach, T. Klüner, A. Groß, *Chem. Phys. Lett.* 376 (2003) 424.
- [7] J.T. Hoefl, M. Kittel, M. Polcik, S. Bao, R.L. Toomes, J.H. Kang, D.P. Woodruff, M. Pascal, C.L.A. Lamont, *Phys. Rev. Lett.* 87 (2001) 086101.
- [8] R. Lindsay, P. Baumgärtel, R. Terborg, O. Schaff, A.M. Brandshaw, D.P. Woodruff, *Surf. Sci.* 425 (1999) L401.
- [9] L. Andersson et al., MOLCAS version 5.4: Quantum Chemistry Software Department of Theoretical Chemistry, Lund University, Lund, Sweden.
- [10] I. Mehdaoui, D. Kröner, M. Pykavy, H.-J. Freund, T. Klüner, in preparation.
- [11] S.F. Boys, F. Bernardi, *Mol. Phys.* 19 (1970) 553.
- [12] R. Wichtendahl, M. Rodriguez-Rodrigo, U. Härtel, H. Kuhlenbeck, H.-J. Freund, *Surf. Sci.* 423 (1999) 90.
- [13] G. Pacchioni, C.D. Valentin, D. Dominguez-Ariza, F. Illas, T. Bredow, T. Klüner, V. Staemmler, *J. Phys. Condens. Matter* 16 (2004) S2497.
- [14] T. Klüner, S. Thiel, H.-J. Freund, V. Staemmler, *Chem. Phys. Lett.* 294 (1998) 413.
- [15] V. Staemmler, *Theor. Chim. Acta* 45 (1977) 89.
- [16] U. Maier, V. Staemmler, *Theor. Chim. Acta* 76 (1989) 95.
- [17] J. Wasilewski, *Int. J. Quantum Chem.* 36 (1989) 503.
- [18] R. Fink, V. Staemmler, *Theor. Chim. Acta* 87 (1993) 129.
- [19] T. Klüner, H.-J. Freund, J. Freitag, V. Staemmler, *J. Chem. Phys.* 104 (1996) 10030.
- [20] P.R. Antoniewicz, *Phys. Rev. B* 21 (1980) 3811.
- [21] M.D. Feit, J.A. Fleck, *J. Chem. Phys.* 78 (1983) 301.
- [22] J.W. Gadzuk, *Surf. Sci.* 342 (1995) 345.
- [23] M. Menges, B. Baumeister, K. Al-Shamery, H.-J. Freund, C. Fischer, P. Andresen, *J. Chem. Phys.* 101 (1994) 3318.